

arXiv:2304.13000v1 [cs.CV] 25 Apr 2023

# Segment anything, from space?

Simiao Ren<sup>1</sup>

cimiao.ren@duke.edu

Francesco Luzi<sup>\*1</sup>

francesco.luzi@duke.edu

Saad Lahrichi<sup>\*2</sup>

saad.lahrichi@duke.edu

Kaleb Kassaw<sup>\*1</sup>

kaleb.kassaw@duke.edu

Leslie M. Collins<sup>1</sup>

leslie.collins@duke.edu

Kyle Bradbury<sup>1,3</sup>

kyle.bradbury@duke.edu

Jordan M. Malof<sup>4</sup>

jordan.malof@umontana.edu

<sup>1</sup> Electrical and Computer Engineering  
Duke University  
Durham, NC 27705<sup>2</sup> Division of Natural and Applied  
Sciences  
Duke Kunshan University  
Kunshan, China 215316<sup>3</sup> The Energy Initiative  
Duke University  
Durham, NC 27705<sup>4</sup> Computer Science  
University of Montana  
Missoula, MT 59801

## Abstract

Recently, the first foundation model developed specifically for vision tasks was developed, termed the "Segment Anything Model" (SAM). SAM can segment objects in input imagery based upon cheap input prompts, such as one (or more) points, a bounding box, or a mask. The authors examined the *zero-shot* image segmentation accuracy of SAM on a large number of vision benchmark tasks and found that SAM usually achieved recognition accuracy similar to, or sometimes exceeding, vision models that had been trained on the target tasks. The impressive generalization of SAM for segmentation has major implications for vision researchers working on natural imagery. In this work, we examine whether SAM's impressive performance extends to overhead imagery problems, and help guide the community's response to its development. We examine SAM's performance on a set of diverse and widely-studied benchmark tasks. We find that SAM does often generalize well to overhead imagery, although it fails in some cases due to the unique characteristics of overhead imagery and the target objects. We report on these unique systematic failure cases for remote sensing imagery that may comprise useful future research for the community. *Note that this is a working paper, and it will be updated as additional analysis and results are completed.*

## 1 Introduction

Foundation models are large deep learning models (e.g., in terms of free parameters) that have been trained on massive datasets, giving them the ability to generalize well to novel down-stream tasks (e.g., novel datasets, or prediction targets) with little or no additional

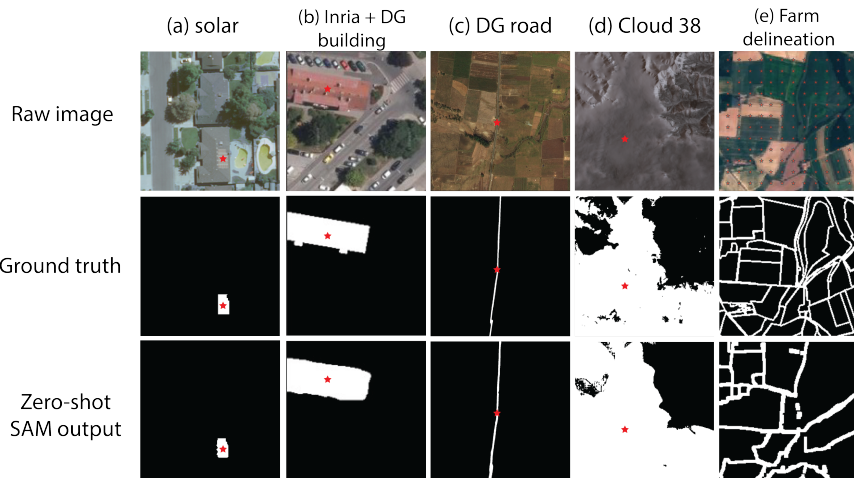


Figure 1: Huge potential in applying SAM [6] into remote sensing field: Illustrative example of the five distinct remote sensing datasets we used and cherry-picked SAM zero-shot result by feeding the prompt illustrated with red stars. In an ideal scenario, zero-shot performance of SAM highly resembles the ground truth segmentation in diverse objects: (a) solar panels (b) buildings (c) roads (d) clouds (e) farm parcel boundaries.

training (i.e., so-called few-shot or zero-shot generalization). Recent foundation models have been focused on natural language processing (NLP) tasks (e.g., BERT [Devlin et al. 2019], GPT-3 [Brown et al. 2020]), while some work also focused upon text and imagery (e.g., CLIP [Radford et al. 2021] and ALIGN [55]). Recently the first foundation model primarily designed for vision tasks was developed, termed the "Segment Anything Model" (SAM) [6]. SAM is designed to output a segmentation mask for an input image based upon one (or several) of the following input prompts: one (or more) points, a bounding box, or a segmentation mask (e.g., one that is coarse). The premise of SAM is that these relatively cheap input prompts provide guidance to the model regarding which object(s) in the input image should be segmented. The input/output structure of SAM is illustrated in Fig. 2(a) for land use segmentation in a satellite image.

As described in [6], based upon these cheap input prompts, the goal of SAM is to effectively segment *any* object in *any* image, without the need for additional task-specific or dataset-specific adaptation (e.g., training). To evaluate this capability of SAM, the authors in [6] reported the segmentation accuracy of SAM on a large and diverse collection of benchmark problems (over 23). They also examined the performance of SAM as a function of the type of prompt provided (i.e., point, multiple points, bounding box). The results showed that SAM performed better as the informativeness of the prompts increased, with single-point prompts (least informative) generally achieving lower accuracies and prompts with multiple points or a bounding box (most informative) achieving higher accuracies. Overall, however, the accuracy of SAM was impressive, even when using a single-point prompt. When using richer prompts, such as bounding boxes, SAM often achieved segmentation accuracy that was comparable, or sometimes even superior to, existing models that had been trained specifically for the target problem under consideration (e.g., often with full target label su-

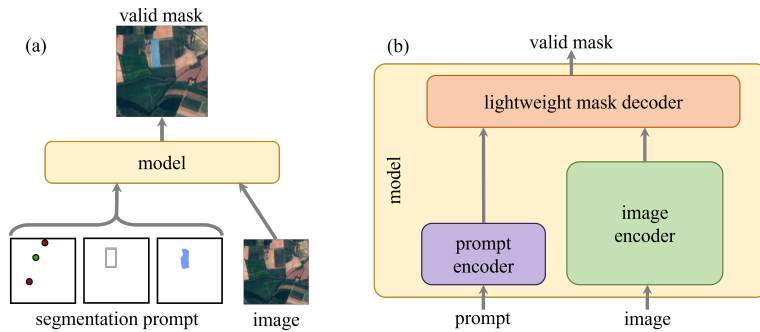


Figure 2: Block diagram of the Segment Anything Model (SAM) for use with satellite imagery. SAM takes as input an image, along with prompts of point coordinates, bounding boxes, and segmentation masks. Figures adapted from the SAM diagram in [5].

pervision) [8]. As a consequence of these findings, SAM is likely to have a major impact on computer vision research and practice. The authors of SAM outline several major areas of future work that may be facilitated or significantly influenced by SAM.

## 1.1 Can SAM Segment Anything, From Space?

In this work we aim to investigate the impact of SAM on vision problems involving overhead imagery, such as imagery collected from satellite, drones, and unmanned aerial vehicles. While the authors of SAM report comprehensive empirical results for SAM, they only consider a single overhead imagery dataset. Overhead imagery problems exhibit unique challenges compared to natural imagery, and therefore it is unclear whether the advantages of SAM will transfer to overhead imagery problems. The goal of this work is to determine whether SAM transfers well to overhead imagery tasks, and thereby provide guidance to the community on how to respond to its development.

To answer this question, we evaluate its segmentation accuracy on a diverse and representative set of tasks involving overhead imagery, and as a function of different prompt types. Such evaluation will reveal the overall quality and reliability of masks generated by SAM under many different practical scenarios. To achieve this goal, we examine the out-of-the-box accuracy of SAM on six existing benchmark datasets of overhead imagery (see Table 1), encompassing 5 million square kilometers of surface area. The benchmarks include a variety of widely-studied object classes (e.g., buildings, roads, cloud cover, farming crops), image resolutions (e.g., 0.3m - 30m), and geographic locations (e.g., including Africa, Europe, Asia, and North America). We also compare SAM’s performance to contemporary vision models that have been trained on each benchmark problem. *We note that this is a working paper, and it will be updated as additional analysis and results are completed.*

## 2 Benchmark Datasets

For our experiments we utilized six benchmark datasets of overhead imagery that were selected for inclusion based upon several criteria. We first had two strict criteria for inclusion:

Dataset	Region	Country	Classes	Size (km <sup>2</sup> )	Resolution (m)	Task
Solar [1]	Fresno	USA	Solar Panel	927.00		
	Stockton	USA		211.50	0.30	Seg
	Modesto	USA		168.75		
	Oxnard	USA		45.00		
Inria [2]	Austin	USA	Building	81		
	Chicago	USA		81		
	Kitsap County	USA		81	0.30	Seg
	West Tyrol	Austria		81		
	Vienna	Austria		81		
DeepGlobe [3]	Las Vegas	USA	Building	150.20		Seg
	Paris	France		41.88		
	Shanghai	China		173.32	0.31	
	Khartoum	Sudan		32.88		
38-Cloud [4]	Earth	-	Cloud	2,188,800	30	Seg
DeepGlobe Roads [5]	-	Thailand	Roads			
	-	Indonesia		2,220	0.50	Seg
	-	India				
Parcel Delineation [6]	-	France	Crop Boundaries	4,403.84	10	Edge

Table 1: A summary of the quantity, resolution, and type of data we evaluate. The resolution is meter per pixel. Task type we have "Seg" for segmentation and "Edge" for edge detection.

(i) the availability of pixel-wise segmentation labels, as these are needed needed to evaluate the performance of SAM and generate input prompts for it; and (ii) the datasets were publicly-available, to enable further study by the community. Among the datasets that satisfied these strict criteria, we also had several soft criteria for inclusion: (i) we prioritized datasets that were of greater interest to the overhead imagery community, as evidenced by their inclusion in many prior or important publications; (ii) benchmarks that involved widely-studied target objects (e.g., buildings, roads, land use); and (iii) datasets that collectively resulted in a representative set of key properties (e.g., geographic location, image resolution, or target classes). The resulting set of six datasets that we selected are shown in Table 1, along with references and key details. Further details about our benchmark datasets can be found in the Supplement.

### 3 Experimental design

The goal of our experiments is to examine whether the impressive performance characteristics of SAM extend to the segmentation of overhead imagery. To do this, we replicate many (but not all) of the experiments reported in the SAM publication [1], with the minimum number of modifications needed to enable experimentation on overhead imagery. Therefore we evaluate the segmentation accuracy of SAM on **each** of our benchmark tasks (summarized in Sec. 2) with respect to varying characteristics of the input prompts, and the way in which the output of SAM is utilized and scored. This results in three major experimental variables that are varied in our experiments: (i) Input Prompt Type, (ii) Prompt Source, and (iii) SAM Mask Selection method. We describe each of these below. The experimental design variables are illustrated in Fig. 3. We finish by discussing major differences between our experiments and those in the SAM paper [1].

**Prompt Type.** The current public version of SAM can accept three types of input

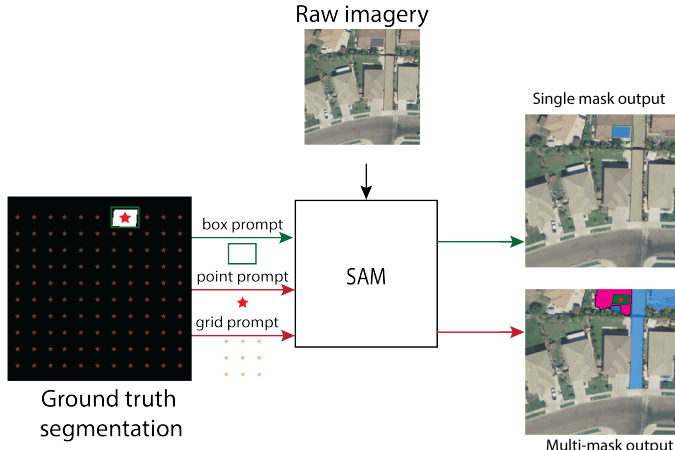


Figure 3: Schematic diagram for our prompt types. Three different prompt types are examined: Bounding Box, Single Point (center/random), Grid Point. For single-point prompts, due to the ambiguity presented, we take all three output masks from SAM. For the bounding box prompt, we use the single mask output mode of SAM.

prompts: one (or many) point coordinates, a bounding box, or a mask. The variable "Prompt Type" indicates which of these prompt input was used in the experiment, and in the case of point-based prompts, the number and spatial arrangement of these prompts with respect to the target object. We summarize each Prompt Type here:

- *Center Point*. A single point prompt that is centered on the target object.
- *Random Point*. A single point prompt that is placed randomly at some location on the target object.
- *Bounding Box*. A single bounding box that approximately represents the extent of the target object in the imagery.
- *Grid Points*. A collection of points that are placed on a regular grid over the input image. This prompt is only used for the edge detection task.

Except for the Grid Points type, all of these prompt types rely on knowledge of the precise location and extent of the target object. Therefore, following the SAM paper [6], we utilize the ground truth segmentation masks to obtain this information and properly set these prompts. In contrast to [6], we exclude mask prompts from our experiments due to difficulties with the proper setting of these values (see Supplement for more details).

**Mask Selection Method.** Mask selection refers to the manner in which the output of SAM is utilized to create a final predicted segmentation mask. The SAM model is designed such that it can produce up to three candidate segmentation masks for a given input prompt. Furthermore, SAM assigns each mask a score indicating the relative likelihood that the mask is appropriate given the image and input prompt. Based upon this output, we consider three different Mask Selection Methods that were also employed in [6]:

- *Max Confidence* We simply take the mask that has the highest confidence score.

- *Oracle* We compare each predicted mask and take the one that is most similar, in terms of intersection-over-union, to the target ground truth mask. This method emulates a human-in-the-loop scenario, such as computer-aided labeling, where a human can evaluate the quality of the masks and choose the best one.
- *Single Output (bounding box prompt only)* We operate SAM in "single output" mode, where it produces a single mask without any confidence score. Note that this is not simply taking the max confidence score among the three candidate masks (see [6]), and instead represents a fundamentally different decoding scheme. Consistent with [6], we only use this Selection Method for Bounding Box prompt types.

### 3.1 Structure of the Experiments

For the subset of experimental designs that we run from [6], our experimental configurations are largely consistent with theirs. For conventional segmentation tasks in overhead imagery - which includes all datasets except for Parcel Delineation - we conduct the same combination of experiments. Specifically, we consider three prompt methods: *Center Point*, *Random Point*, and *Bounding Box*. For the two point-based prompt methods, we consider two mask selection techniques: *Max Confidence*, and *Oracle*. For the *Bounding Box* prompt method we only consider the *Single Output* mask selection setting, as it was designed for this setting.

The Parcel Delineation Dataset is designed for edge detection, and therefore we use a different experimental design, closely resembling the same edge detection experiment from [6]. The task for this dataset is to identify the edges separating different parcels of land. To achieve this goal, one must segment each unique parcel (i.e., object) in the imagery, and then extract the boundaries between the parcels. To accomplish this, we use a Grid Point prompt method to extract masks for all parcels in the input image. We then use a Canny Edge detector to extract edges at the boundaries between parcels and compare this with the ground truth parcel edge masks that accompany the dataset. Full details of the edge extraction process can be found in the Supplement.

### 3.2 Baseline Task-specific models

For a given benchmark problem we also report the segmentation accuracy of two "task specific models"; these models are been trained with full supervision on that benchmark. Specifically, we compare SAM to a U-Net model [6] that has been highly optimized for the benchmark in a prior study. We refer to this as "UNet-Opt" and it approximates the state-of-the-art performance that can be achieved on that benchmark, given substantial investment. For the Unet-Opt model we report the results reported in a prior study involving the particular benchmark under consideration. We also compare SAM with a conventional Unet model that we have trained here, reflecting the accuracy achievable without substantial investment, but assuming the availability of (often substantial) labeled training data. We refer this model as "UNet".

### 3.3 Scoring Procedure

Following [6, 7, 8], we report pixel-wise IOU of our mask predictions, which is given by  $IOU = |\hat{T} \cap T| / |\hat{T} \cup T|$ . Here  $\hat{T}$  is the set of pixels predicted to be in the mask (value of 1), while  $T$  is the set of ground truth pixels (value of 1) in the true mask. In this regime,

both  $T$  and  $\hat{T}$  encompass all pixels the entire dataset, and no distinction is made between the masks of individual target objects, or so-called instance masks, which we denote  $T_i$  for the  $i^{th}$  object. However, SAM was primarily designed for instance segmentation, whereby it aims to make predict  $T_i$  rather than  $T = \cup_i T_i$  given a single input prompt. To address this problem, and score SAM more fairly, we identify all connected components in our dataset and treat them as masks for individual target instances. We use these masks to extract prompts for SAM (e.g., point or bounding box), and then collect the predictions for each input prompt, denoted  $\hat{T}_i$ . To obtain a global mask with which to score SAM we take the union of all of its instance predictions  $\hat{T} = \cup_i \hat{T}_i$ . Note that this strategy is imperfect since our instance masks may contain multiple instances in some cases (e.g., neighboring houses with different roof colors) and SAM may tend to underestimate the masks (see Supplement), however, we find that this strategy works reasonably well.

## 4 Experimental Results

The results of our experiments are reported in Table 2. The main goal of our experiments is to answer the following question: can SAM segment anything from space? A high-level response to this question can be found in Section 5. We assert that SAM can indeed segment anything from space, if it achieves (i) high overall accuracy on our benchmark tasks, and (ii) achieves consistent accuracy across the tasks. Therefore, in this section we address these two questions in detail, informed by our experimental results.

Model	Prompt Method	Mask Selection	Solar	Inria + DG (Building)	DeepGlobe (Roads)	38-Cloud	Parcel Delineation	Parameters (M)
Unet-Opt	NA	NA	81.05 [1]	79.53 [1]	62.94 [1]	86.08 [1]	36.99 [1]	104.89
Unet	NA	NA	78.39	72.50	58.35	72.88	-	
SAM [1]	Center Point	Max confidence	48.18	40.40	7.24	65.64	-	
	Center Point	Oracle	74.17	64.41	11.53	78.63	-	
	Random Point	Max confidence	39.96	36.76	7.17	64.70	-	
	Random Point	Oracle	64.19	61.01	11.41	77.46	-	636
	Bounding Box	Single output	81.12	69.61	7.47	86.48	-	
	Grid points	Max confidence	-	-	4.5	-	10.1	

Table 2: (pixel) Intersection-over-union (IoU) for each experimental scenario considered

### 4.1 Overall accuracy of SAM

In the context of machine learning, this question is typically answered by comparison of competing models; in this case we compare SAM to two contemporary task-specific models (see Sec. 3). The results in Table 2 indicate that the accuracy of SAM depends strongly upon the prompt that it is provided, with richer prompts (e.g., bounding box rather than a single point) generally yielding greater segmentation accuracy. However, SAM often achieves impressive segmentation accuracy using either point prompts or bounding boxes. On the Solar and 38-Cloud dataset, SAM achieves comparable performance to the Unet-Opt and Unet models using only a single point prompt (using "Oracle" selection to remove object ambiguity). On these same benchmarks SAM achieves *superior* performance to the highly optimized Unet-Opt model when prompted with a bounding box - this is impressive since SAM was not trained or optimized for these tasks. In fact, presumably SAM has not been

trained on any imagery of this kind, yet it can perform similar to highly optimized models that have been trained specifically for these tasks. As discussed next however, SAM does not achieve such strong results on all of the benchmarks.

## 4.2 Domain-robustness of SAM

The accuracy of SAM varies substantially across our benchmark problems. While it achieves impressive results on the Solar and 38-Cloud benchmarks, its accuracy is more modest on the Inria+DG (building) benchmark. On the building task it does not outperform either of the task-specific models (Unet and Unet-Opt), even when using a bounding box prompt. However, it does achieve comparable accuracy to the Unet model when using the Bounding Box prompt, suggesting that it still generalizes reasonably well considering the visual complexity and heterogeneity of buildings. Furthermore, the task-specific models in these cases are trained using relatively large and diverse training datasets that are representative of the target datasets. Lastly, we find that SAM may be disadvantaged by limitations of our ground truth labels, which may include multiple buildings, even though SAM is trained to segment a single instance of a target class (see Section 3). If corrected, SAM may perform much more closely to the task-specific models, however, this limitation of the ground truth is difficult to overcome.

SAM performs very poorly on both Road Segmentation and Parcel Delineation. In these cases SAM performs substantially worse than the task-specific models, regardless of the prompt employed. Note that in the case of Parcel Delineation, only the *Grid Points* prompt was applicable, since we needed to segment all parcels in the input image. The challenges associated with the Parcel Delineation are similar to those reported for edge detection tasks (to which Parcel Delineation belongs) in the original SAM publication [6], where it was found that SAM tends to over-segment the parcels, resulting in overall poor IOU. We observe the same tendency on our Parcel Delineation benchmark. It is also notable that the Parcel Delineation problem is challenging overall; the task-specific model performs much more poorly on this problem than comparable task-specific models on other problems, suggesting it is intrinsically more difficult. This may reflect the difficulty in defining where one parcel ends and another begins.

The road segmentation benchmark problem presents several challenges for SAM that may be somewhat unique to overhead imagery. First, SAM is designed to segment individual instances of objects, however, the notion of an object *instance* is not well-defined for some classes of objects in overhead imagery. For example, the notion of an instance implies that there is some well-defined physical extent to an object, however, roadways are connected across vast geographic areas. Although the visual features of a road may change over space they are usually given the same mask (as in the case of our benchmarks); in these cases SAM often isolates a visually homogenous subset of the roadway as being a unique road instance, for which it is penalized (detailed results pending).

Another systematic limitation of SAM that we find is its sensitivity to occlusion. Occlusion is still considered a major challenge in vision problems more broadly, and we find that SAM is still vulnerable to occlusion. This limitation of SAM is most apparent in road segmentation, where the roadways are often occluded by vehicles, buildings, or trees. Often these occlusions span the width of roadways, creating visually disconnected portions of roadway, and SAM treats these as separate roadway instances, and is penalized heavily for generating an incomplete segmentation mask.

## 5 Conclusion: Can SAM Segment Anything, From Space?

The simple answer to this question is "no", not when used out-of-the-box, without any modification or additional training. However, SAM does achieve impressive results on several tasks, without the benefit of much (if any) training on overhead imagery tasks. SAM often achieves accuracy comparable, or superior to, the performance of *task-specific models*, which are models that have been trained and heavily optimized (e.g., its hyperparameters) on the task under consideration. This indicates that SAM may be an impactful vision model for many tasks in overhead imagery, even if it isn't (yet) consistently effective for all tasks. Furthermore, when SAM does fail on a task, we find that it may be due to specific systemic failures that may conceivably be addressed through modest changes in SAM's design, or training procedure, to adapt it to overhead imagery problems. If these limitations can be addressed, it may enable SAM (or related models) to achieve high accuracy across a wide range of overhead imagery tasks, resulting in major implications for vision research on overhead imagery.

## References

- [1] Han Lin Aung, Burak Uzkent, Marshall Burke, David Lobell, and Stefano Ermon. Farm parcel delineation using spatio-temporal convolutional networks. In *Proceedings of the IEEE/CVF Conference on Computer Vision and Pattern Recognition Workshops*, pages 76–77, 2020.
- [2] Han Lin Aung, Burak Uzkent, Marshall Burke, David Lobell, and Stefano Ermon. Farm Parcel Delineation Using Spatio-temporal Convolutional Networks. In *2020 IEEE/CVF Conference on Computer Vision and Pattern Recognition Workshops (CVPRW)*, pages 340–349, Seattle, WA, USA, June 2020. IEEE. ISBN 978-1-72819-360-1. doi: 10.1109/CVPRW50498.2020.00046. URL <https://ieeexplore.ieee.org/document/9150690/>.
- [3] Gaétan Bahl, Lionel Daniel, Matthieu Moretti, and Florent Lafarge. Low-power neural networks for semantic segmentation of satellite images. In *Proceedings of the IEEE/CVF International Conference on Computer Vision Workshops*, pages 0–0, 2019.
- [4] Kyle Bradbury, Raghav Saboo, Timothy L Johnson, Jordan M Malof, Arjun Devarajan, Wuming Zhang, Leslie M Collins, and Richard G Newell. Distributed solar photovoltaic array location and extent dataset for remote sensing object identification. *Scientific data*, 3(1):1–9, 2016.
- [5] Ilke Demir, Krzysztof Koperski, David Lindenbaum, Guan Pang, Jing Huang, Saikat Basu, Forest Hughes, Devis Tuia, and Ramesh Raskar. Deepglobe 2018: A challenge to parse the earth through satellite images. In *Proceedings of the IEEE Conference on Computer Vision and Pattern Recognition Workshops*, pages 172–181, 2018.
- [6] Alexander Kirillov, Eric Mintun, Nikhila Ravi, Hanzi Mao, Chloe Rolland, Laura Gustafson, Tete Xiao, Spencer Whitehead, Alexander C. Berg, Wan-Yen Lo, Piotr Dollár, and Ross Girshick. Segment Anything, April 2023. URL <http://arxiv.org/abs/2304.02643>. arXiv:2304.02643 [cs].

---

- [7] Francesco Luzi, Aneesh Gupta, Leslie Collins, Kyle Bradbury, and Jordan Malof. Transformers for recognition in overhead imagery: A reality check. In *Proceedings of the IEEE/CVF Winter Conference on Applications of Computer Vision*, pages 3778–3787, 2023.
- [8] Emmanuel Maggiori, Yuliya Tarabalka, Guillaume Charpiat, and Pierre Alliez. Can semantic labeling methods generalize to any city? the inria aerial image labeling benchmark. In *IEEE International Geoscience and Remote Sensing Symposium (IGARSS)*. IEEE, 2017.
- [9] Emmanuel Maggiori, Yuliya Tarabalka, Guillaume Charpiat, and Pierre Alliez. Can semantic labeling methods generalize to any city? the inria aerial image labeling benchmark. *2017 IEEE International Geoscience and Remote Sensing Symposium (IGARSS)*, 07 2017. doi: 10.1109/igarss.2017.8127684.
- [10] S. Mohajerani, T. A. Krammer, and P. Saeedi. "A Cloud Detection Algorithm for Remote Sensing Images Using Fully Convolutional Neural Networks". In *2018 IEEE 20th International Workshop on Multimedia Signal Processing (MMSP)*, pages 1–5, Aug 2018. doi: 10.1109/MMSP.2018.8547095.
- [11] Spencer Paul, Ethan Hellman, and Rodri Neito. Solarx: Solar panel segmentation and classification.
- [12] Olaf Ronneberger, Philipp Fischer, and Thomas Brox. U-net: Convolutional networks for biomedical image segmentation. In *Medical Image Computing and Computer-Assisted Intervention–MICCAI 2015: 18th International Conference, Munich, Germany, October 5-9, 2015, Proceedings, Part III 18*, pages 234–241. Springer, 2015.
- [13] Lichen Zhou, Chuang Zhang, and Ming Wu. D-linknet: Linknet with pretrained encoder and dilated convolution for high resolution satellite imagery road extraction. In *Proceedings of the IEEE Conference on Computer Vision and Pattern Recognition Workshops*, pages 182–186, 2018.